Probing alamethicin channels with water-soluble polymers

Effect on conductance of channel states

Sergey M. Bezrukov*‡ and Igor Vodyanoy§

*University of Maryland, College Park, Maryland 20742, and National Institutes of Health, Biophysics Unit, Laboratory of Biochemistry and Metabolism/National Institute of Diabetes and Digestive and Kidney Diseases, Bethesda, Maryland 20892; and §Office of Naval Research, Arlington, Virginia 22217-5000, Laboratory of Biochemistry and Metabolism/National Institute of Diabetes and Digestive and Kidney Diseases, Bethesda, Maryland 20892, and Department of Physiology and Biophysics, University of California, Irvine, California 92717 USA

ABSTRACT Channel access resistance has been measured to estimate the characteristic size of a single ion channel. We compare channel conductance in the presence of nonpenetrating water-soluble polymers with that obtained for polymer-free electrolyte solution. The contribution of the access resistance to the total alamethicin channel resistance is ~10% for first three open channel levels. The open alamethicin channel radii inferred for these first three levels from the access resistance are 6.3, 10.3, and 11.4 Å.

The dependence of channel conductance on polymer molecular weight also allows evaluation of the channel dimensions from polymer exclusion. Despite varying conductance, it was shown that steric radii of the alamethicin channel at different conductance levels remain approximately unchanged. These results support a model of the alamethicin channel as an array of closely packed parallel pores of nearly uniform diameter.

INTRODUCTION

The use of water-soluble polymers to study ionic channels provides new methods for obtaining information on channel dimensions and their change during transitions of the channel between different conductance states. Osmotic stress by polymers excluded from channel interior was first used by Zimmerberg and Parsegian (1), who studied the voltage-dependent anion channel from the outer membrane of mitochondria. Channels under osmotic stress tend to collapse the polymer inaccessible aqueous volume. The decrease in probability of the open state on application of osmotic pressure provided an estimate of the volume change at channel transitions between open and closed states. This approach was subsequently used to determine the change in volume of potassium channels of the squid giant axon (2).

Water-soluble polymers not only introduce various osmotic effects but also increase the viscosity of solutions and decrease their macroscopic (bulk) conductivity. The change in the microscopic conductivity depends on the scale and particular structure of the conductor. For example, small ionic channels with interiors inaccessible to solutes should not undergo significant conductance change. In contrast, the conductance of big aqueous pores easily penetrable by polymer molecules should change in parallel with bulk electrolyte conductivity. This effect has been used for sizing toxin-induced channels (3) and alamethicin channels (4, 5).

We describe experiments on the alamethicin-induced conductance of lipid bilayers in the presence of water-soluble polymers polyethylene glycols and dextran. Alamethicin, a 20 amino-acid peptide, has been studied for some years as a model for voltage-gated channels (6), the main reason for enduring interest being the strong voltage dependence of alamethicin-induced conductance. Single-channel properties of alamethicin channels have been studied extensively by several groups (7–9) (for review see reference 10).

In the present article, we restrict ourselves to analysis of the effects of solution conductivity changes caused by addition of polymer solutes. We show that steric considerations based on characteristic polymer sizes in solution and access resistance measurements for nonpenetrating, excluded polymers allow us to evaluate channel dimensions using these two completely independent approaches. Analysis of noise in the open alamethicin channel in the presence of penetrating polymers is used to derive some conclusions on the mechanism of polymer action.

Our data also yield information on the influence of polymers on channel kinetics and probabilities of different conductive levels. The osmotic-stress effects that provide an independent way of channel sizing (1) and the viscosity-induced changes in kinetics will be discussed elsewhere.

MATERIALS AND METHODS

"Solvent-free" membranes were prepared as described by Montal and Mueller (11). The membrane forming solution was L-alpha-diphytanoyl lecithin (Avanti Polar Lipids, Inc., Pelham, AL) in *n*-pentane (5 mg/ml). The chamber, developed in the laboratory of James Hall (Irvine, CA) (12), was made from Teflon. Two symmetrical halves with volumes of 3 cm^3 were divided by 15 μm Teflon partition with round aperture of ~100 μm diameter. Hexadecane in *n*-pentane (1:10) was used for the aperture pretreatment. Alamethicin purified as described in Balasubramanian et al. (13) was added to membrane bathing solution from ethanolic stock solutions after bilayer formation. Analytical grade sodium chloride from Mallinckrodt, Inc. (Paris, KY) was used to prepare aqueous stock solutions of 1.0 M concentration buffered at pH 6.2 by MES (mol wt 213.2) from Calbiochem Corp. (La Jolla, CA).

‡ On leave from St. Petersburg Nuclear Physics Institute of the Russian Academy of Sciences, Gatchina, 188350 Russia.

Address correspondence to Dr. I. Vodyanoy, Office of Naval Research, 800 N. Quincy St., Arlington, VA 22217-5000.

0006-3495/93/01/016/10 $2.00

Polyethylene glycols (PEGs) of different molecular weights from Aldrich Chemical Co., Inc. (Milwaukee, WI) and dextran 17,900 from Sigma Chemical Co. (St. Louis, MO) were used to obtain needed weight/weight concentration. To keep the ion/water molar ratio constant, the polymers were added to NaCl stock solutions. In several experiments, PEGs from Fluka (Buchs, Switzerland) were used, namely Carbowax 20000, Carbowax 1540, and Carbowax 400. No difference in PEG-induced effects was found. Bulk electrolyte conductivity was measured using a conductivity meter (model CDM 80; Radiometer, Copenhagen, Denmark).

A pair of Ag-AgCl electrodes with agar bridges was used to maintain membrane potentials and to pick up current fluctuations. Electrodes and bridges were assembled within standard 200-μl pipette tips using agar boiled in 3 M NaCl aqueous solution and silver wires of 1 mm diameter pretreated by immersing in 0.1 HCl at direct current of 0.5 mA/cm^2 density for 3 h. The input amplifier was 3902 headstage (a 10^8 Ω feedback resistor, max input current 10^{-7} A) of the 3900 integrating patch-clamp system (Dagan Corporation, Minneapolis, MN). All input circuits and two pairs of syringes for membrane formation and bathing solution changing were placed within a double high-μ metal screen (Amuneal Manufacturing Corp., Philadelphia, PA) that provided $>10^4$-fold damping of magnetic and electric stray field components in noise spectra.

Current fluctuations were recorded with the help of the digital magnetic tape recorder Unitrade/Toshiba DX-900 (DAS-900; Unitrade, Philadelphia, PA) operated in Pulse Code Modulation mode. Recorded data were then analyzed using a Gateway 2000 80386/387 33 MHz computer (Gateway 2000, North Sioux City, SD) with the Adalab-PC 12 bit A/D converter board that could be operated at 100–40,000-Hz sampling frequency. Single-channel statistics and conductance levels were determined after signal filtering by an 8-pole Bessel filter (Frequency Devices 902; Frequency Devices, Haverhill, MA) with 1.5 or 2.5 kHz corner frequencies. In noise measurements, an 8-pole Butterworth filter (Frequency Devices 901) was used, the corner frequency being chosen equal to three-eighths of the sampling frequency. Fourier transformations were made on 2048 point vectors.

To measure noise of the open channel, i.e., the noise of the current through the channel during the segments of recordings corresponding to a specific conductance level (Fig. 1), we used a special pretreatment of current recordings. Segments of recordings corresponding to a chosen level of pore conductance were selected and, after cutting 250 μs off both ends of the segment to eliminate transition phenomena and zeroing of the mean value of the segment, were used to obtain 2,048-point vector for spectral density evaluations. Several tests were performed to exclude the possibility of spectrum distortion due to a limited lifetime of the channel at a specific conducting level. In one of them, a signal from a calibrated external noise generator was mixed into the channel current recording. Spectra obtained from this signal were then compared with those measured directly from the output of the noise generator. It was found that the damping of the admixed signal spectra is significant only at the lowest frequencies of the range, i.e., at frequencies < 60 Hz.

The design of the chamber permitted the change of membrane bathing solutions without damaging the membrane. In a typical experiment, a bilayer was first formed by raising solutions in both chamber compartments 2 mm above the opening in the partition. Membrane capacitance was measured to be 30–50 pF. Magnetic stirring was then started, and alamethicin was added to the front compartment of the chamber, membrane voltage being switched to 100 mV (alamethicin side positive). This voltage was used throughout all experiments if not stated otherwise. After 10 or 20 min, single channels began to appear, and after 30 min their behavior looked stationary. Then, the stirrers were switched off, and the tape recorder was started to obtain 10 or 20 min of "control" recording. After that, using two additional syringes of 5 cm^3 volume, the bathing solution near the membrane was changed by slowly replacing initial electrolyte with heavier and more viscous polymer-containing solution added from the bottom of chamber compartments. The change of bathing solution took ~0.5 min. Another 10 min of recording were obtained. The procedure of electrolyte change could then be reversed to verify the absence of mixing between two phases. The absence of mixing was additionally checked, putting dyes into the second phase and repeating the procedure of solution change several times. All measurements were made at room temperature, 22–23°C.

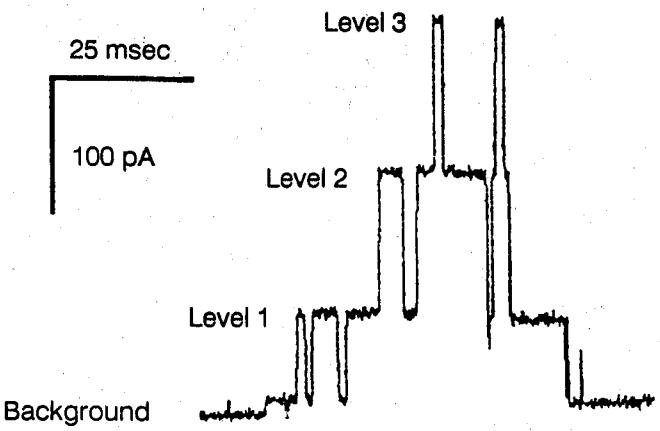

FIGURE 1 A sample of the single-channel recording at 100 mV membrane voltage. The conductance levels are numbered according to the convention of this article.

RESULTS

An example of current steps generated by a single alamethicin channel is shown in Fig. 1. The conductance fluctuations appear in bursts containing channel transitions between several conducting states (7–10). The current bursts always appeared and disappeared through the lowest conducting state, the "0-state" (8, 14). The conductances of different states were nearly ohmic (slightly superlinear at voltages larger than 100 mV), and the states were not integral multiples of each other. We were able to distinguish up to five such states (including the "0-state"), but states corresponding to level 4 and possibly higher levels were rarely seen. For these levels, it was difficult to obtain good statistics. The probability of finding a channel at 0-state was high enough, but relatively small conductance of the channel in this state precluded an accuracy adequate for analysis. Therefore, we restricted our consideration to the levels 1, 2, and 3.

Raw data were obtained as histograms of membrane current. Fig. 2 presents such histograms for several different concentrations of PEG 400. The conductance of all levels decreases as concentration of the polymer increases.

A comparison of PEG effect on channel conductance and on bulk solution conductivity is shown in Fig. 3. The points for a certain level of channel conductance were obtained as ratios of the level conductance in PEG-containing solution to that in polymer-free solution, the experiment with polymer-free solution being done first, as described in the previous section. The conductance of a level was determined as the mean value averaged over

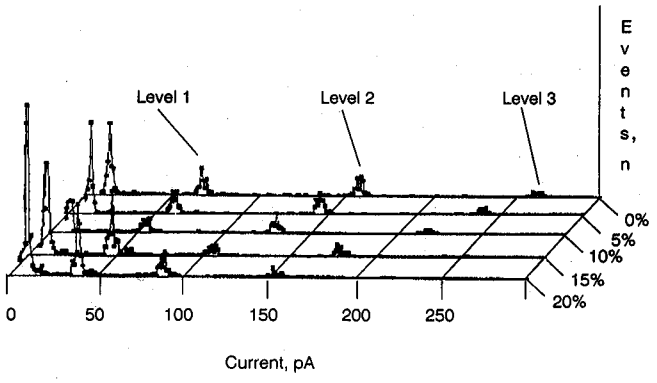

FIGURE 2 A histogram of the membrane single-channel current in the presence of different concentrations of PEG 400. PEG concentration is shown as a weight/weight percents in Z axis of the three-dimensional histogram. In the left-hand side, out-of-scale peaks corresponding to the background membrane current are deleted to clarify the picture. Current reduction with increasing polymer concentration is accompanied by a redistribution of level probabilities in favor of lower conducting states due to osmotic effects. These effects will be considered in a forthcoming article.

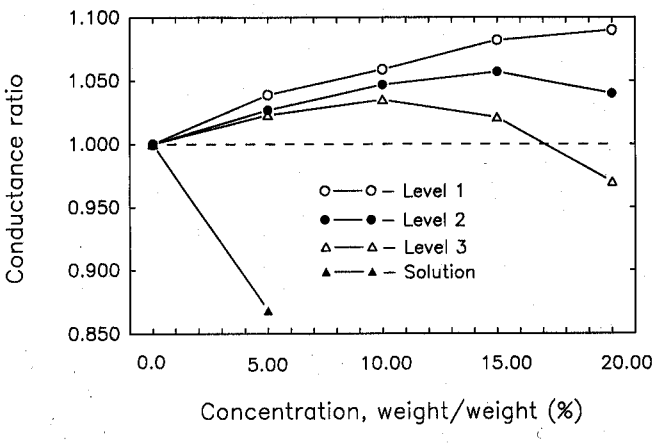

FIGURE 4 The ratio of channel conductance in the presence of PEG 3,400 to channel conductance in polymer-free solution (h^*_{mn}/h_{mn}) as a function of the polymer concentration. The dashed line corresponds to the unchanged channel conductance. Note that an addition of small amounts of PEG 3,400 to 1 M NaCl solution increases single-channel conductance.

corresponding peak of a histogram (see Fig. 2) minus conductance of "bare" membrane.

For solutions of PEG 400 (Fig. 3), the approximate reduction in conductance of channel levels is close to the PEG-induced reduction in bulk electrolyte conductivity. This is not true for solutions of larger PEG 3,400 molecules. The effect shown in Fig. 4 is not only much smaller but is opposite in direction. For example, a 5% concentration of PEG 3,400, which reduces the bulk electrolyte conductivity to the same degree as does PEG 400, actually increases channel conductance. An increase in polymer concentration up to 15% produces an increase in conductance for all three levels studied.

The dependences of the conductance ratios on PEG size are shown in Fig. 5. The polymer concentration is fixed at 15% (wt/wt) for all points. This concentration results in a 0.61 ± 0.01 ratio of bulk electrolyte conductivity decrease. For the smallest PEG used in our study (PEG 200), the effect on channel conductance is close to that on bulk electrolytes. But as polymer size increases, the reduction of conductance diminishes, and in polymer weights of ~2,000, an increase in channel conductance is observed. Larger PEGs at this concentration increase the conductance of the levels more effectively. Hydrodynamic PEG radii (Å) shown inside Fig. 5 are taken from Kuga (15), where they were obtained from viscosity numbers or diffusion coefficients.

The effect of dextran 17,900 on bulk electrolyte conductivity is similar to that of PEGs, but the effect on channel conductance is quite different. Fig. 6 shows only

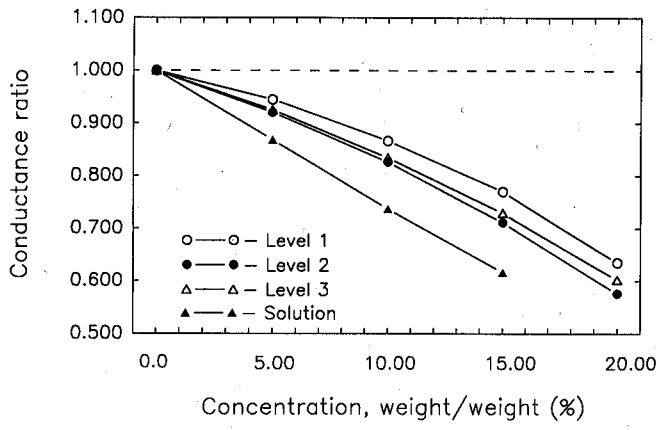

FIGURE 3 The ratio of channel conductance in the presence of PEG 400 to channel conductance in polymer-free solution as a function of the polymer concentration. This ratio is denoted as h^*_{mn}/h_{mn} in the discussion. The dashed line corresponds to the unchanged channel conductance.

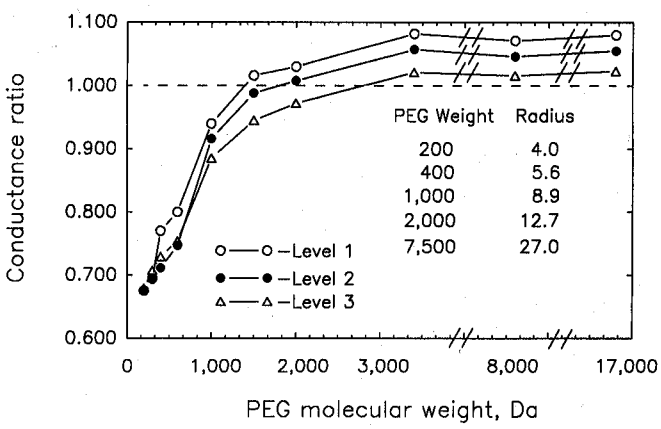

FIGURE 5 The dependence of a PEG-induced channel conductance change (h^*_{mn}/h_{mn}) on the polymer weight. The dashed line corresponds to the unchanged channel conductance. Polymer hydrodynamic radii obtained from viscosity numbers or diffusion coefficients (15) are given in angstroms.

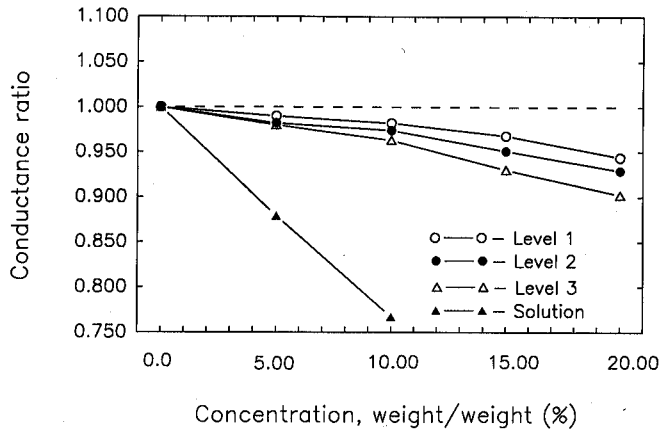

FIGURE 6 The ratio of channel conductance in the presence of dextran 17,900 to channel conductance in polymer-free solution (h^*_{mn}/h_{mn}) as a function of the polymer concentration. The dashed line corresponds to the unchanged channel conductance. Note that dextran induces only monotonic decrease in single-channel conductance.

a monotonic decrease of level conductances with increasing dextran concentration. The effect is rather moderate compared with that of small PEGs.

DISCUSSION

Steric considerations

We first examine the PEG-induced channel conductance change versus polymer molecular weight. Disregarding for now the increase in conductance of levels for large polymers, one can see that at constant polymer concentration the channel conductance is polymer-weight dependent only for small polymers with molecular weights < 3,000 (Fig. 5). For the smallest polymer used, the conductance of all studied levels drops approximately in the same proportion as that of bulk electrolyte. This effect diminishes with the polymer size. It should be stressed here that for a given PEG volume fraction, bulk conductivities of solutions were the same for all PEGs used, the difference for polymers of different weights being within 2%. This means that the dispersion in the curves is due to a polymer-channel interaction.

A simple approach to the problem consists of regarding random polymer coils as flexible spheres of corresponding average hydrodynamic radius. Then, as illustrated in Fig. 7 *A*, sufficiently large PEGs cannot penetrate channels due to steric reasons and thus do not influence the intrinsic channel conductance to substantial degree. For PEGs of smaller sizes, a certain possibility of polymer penetration into the channel arises, and the picture becomes more complex. At the opposite limit, i.e., for polymers much smaller than a channel diameter, the picture is rather simple again. If properties of the solution within the channel and in the bulk are the same, then we will have uniform distribution of polymer, including the channel interior. Here, microviscosity on the scale relevant to an ion friction will be the same all along the ion current path (Fig. 7 *B*), and conductance of the system electrolyte-channel-electrolyte on the addition of a polymer should change in the same proportion as bulk solution conductivity. Results for PEG 200 are in a good agreement with such a conclusion.

Most complicated is the case of intermediate polymer sizes. The solute molecules can exchange their hydration shell of water molecules for chemical groups of the channel hydrophilic interior, so that in interpreting the results of these experiments one may need to consider the radius of the dehydrated form of the penetrating molecule that may be significantly different from Stokes radius (16). Moreover, even an equilibrium distribution of polymer molecules between bathing solution and the channel interior is not a well-developed problem. To our knowledge, explicit calculations of entropic effects have been made only for a random polymer coil between two parallel plates in two limiting cases when a distance between the plates is much smaller or much bigger than the radius of the coil (17). Certainly, it also applies to the dynamics of the polymer passage through the channel.

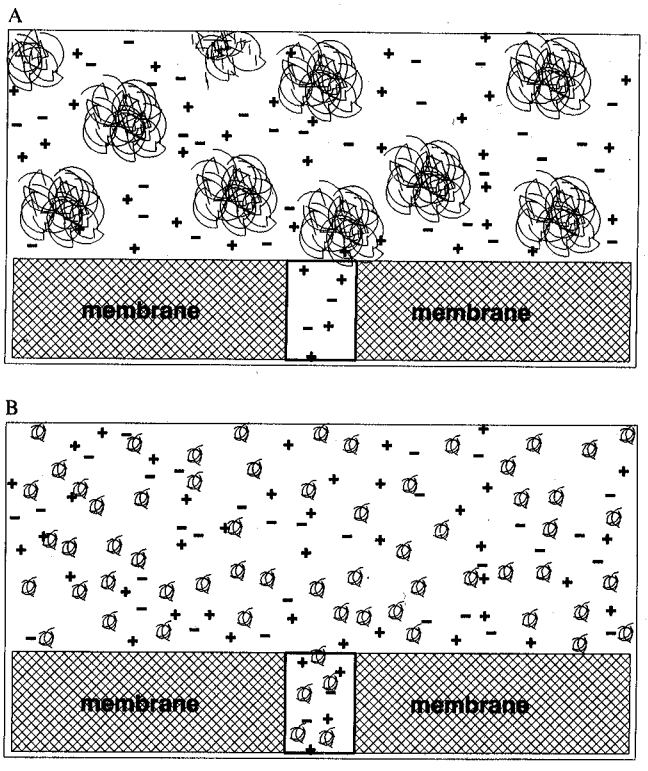

FIGURE 7 (*A*) A cartoon showing the alamethicin channel in the presence of a large polymer. The large polymer coils do not penetrate the channel and thus do not change its conductance significantly. (*B*) A cartoon showing the alamethicin channel in the presence of a small polymer. The small polymer coils are uniformly distributed in solution including the channel interior. The conductance of this system should scale with a bulk solution conductivity.

One can imagine several possible mechanisms of channel conductance reduction in the presence of polymers of intermediate sizes. In principle, the action of polymers with coil dimensions close to the pore diameter may be similar to that of well-known molecular blockers of smaller ionic channels (18). For example, amphotericin B channels in lipid bilayers are blocked by a variety of neutral and charged molecules, the most important condition of effective blocking being correspondence between blocker size and the channel entrance (19). Blocking molecules completely close the channel during a characteristic time in the range 10^{-1} to 10^{-3} s depending on particular molecule and, for charged blockers, on membrane voltage. Time constants in the range 10^{-1} to 10^{-5} s were found for molecular blockers of native ionic channels (18, 20, 21). The reduction in conductance was accompanied by the rise of an intensive blocker-induced noise component in membrane current.

On the other hand, the action of water soluble polymers on the alamethicin channel may be quite different from that discussed above because of the flexibility of the polymer coil. Due to this flexibility, there may be no specific interactions between the pore and the polymer, so that the channel conductance drop would be well described by an increase in microviscosity of the solution within the pore.

To obtain additional kinetic information, we performed noise measurements on the open channel. Spectral estimates for the current noise of the channel in polymer-free solution were nearly frequency independent in the 40–4,000-Hz range and slightly decreased with increase in the level number (22; Webb, W. W., and D. D. Mak, private communication). The magnitude of fluctuations in the channel was several times larger than one would expect for shot noise.

Addition of polymers further increased the open channel noise. Fig. 8 presents a spectrum of current noise of level 3 in the presence of 15% PEG 400 in comparison with background noise obtained from the segments of the same recording not containing open channels. The spectrum corresponding to PEG-free solution is shown by the interrupted line only in order not to obscure the figure. It can be seen that the polymer induces a "white" noise component of small magnitude comparable with that of the open channel noise. This finding is in a sharp contrast to results for channel blockers, where strong additional noise was reported even at the multichannel level (18, 20, 21).

We estimate characteristic time of channel "blocking" by PEG, considering, for simplicity, a very crude model in which polymer molecule completely closes the channel on entering it. We further assume that only one polymer molecule can be in the channel at a given moment. Then, using results obtained elsewhere (21, 23, 24) for the spectral density of polymer-induced noise, we can write

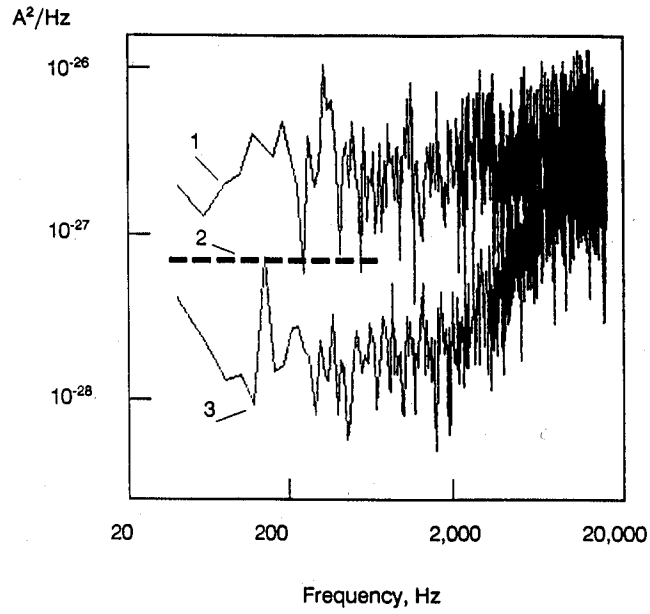

FIGURE 8 Spectral density of the open channel noise (level 3) at 150 mV of membrane voltage. The noise in the presence of 15% of PEG 400 (*curve 1*) exceeds the noise of the channel in the polymer-free solution (*dashed line 2*). The bottom curve (*curve 3*) shows the background noise obtained from the parts of the current recordings when the channel was closed.

$$S_i(f) = 4i^2 \frac{\tau}{\tau_o + \tau_c} \frac{\tau}{1 + (2\pi f\tau)^2}, \quad (1)$$

where i is the current through the open channel, τ_o is the mean open time of the channel, τ_c is the mean time in the closed state, and

$$\tau = \frac{\tau_o \tau_c}{\tau_o + \tau_c}. \quad (2)$$

Without the frequency-dependent term in the denominator of the right-hand side of Eq. 1, we obtain a low-frequency spectral density limit $S_i(0)$. Introducing a "blocking" coefficient,

$$B = \frac{\tau_c}{\tau_o + \tau_c}, \quad (3)$$

we arrive at the expression

$$\tau_c = \frac{1}{B(1-B)^2} \frac{S_i(0)}{4i^2}. \quad (4)$$

For ~30% "block," the mean time in the closed state should be approximately half that in the open state. This degree of block is apparently obtained in level 3 for 15% concentration of PEG 400 (Figs. 4 and 6). Using other known from the experiment values in Eq. 4, we obtain $\tau_c \approx 5 \cdot 10^{-8}$ s. Despite the obvious shortcomings of this model, the estimate for τ_c is of the same order with the

time it takes for 6-Å radius polymer to diffuse a distance of 50 Å. Based on this result, we conclude that in the PEG-alamethicin pore system there is no specific interaction of the type that exists between blocker molecule and ionic channel (18). The drop in pore conductance is well described by the increase in microviscosity of the solution inside the pore, the molecular events being very fast in accord with the time scale of corresponding diffusion rates.

We conclude that polymers with molecular weights below 400 and, correspondingly, with coil radii below 5.6 Å penetrate alamethicin channel easily, because the ratio of channel conductance is close to the ratio of bulk solution conductivities (Figs. 3 and 5), and mobility of these polymers within the channel lumen is comparable with their mobility in a free solution.

Access resistance considerations

The ohmic behavior of alamethicin channel levels reported earlier (8, 10) and their scaling with bulk conductivity for small polymers found in the present article allow us to treat the channel as a macroscopic aqueous pore. Now we will consider the splitting of curves in Fig. 5, i.e., we will try to understand why the effect of polymer is different for different channel levels. For penetrating polymers, the difference can naturally be explained using steric considerations presented above. For a given penetrating polymer, the effect should be stronger for higher conductance level as a result of larger channel radius and, consequently, larger partition of the polymer into the channel interior.

For large nonpenetrating polymers, this explanation is no longer valid, so we will incorporate the notion of channel access resistance. The value of access resistance that adds to the resistance of the channel proper may be written using the conductivity of the bulk solution σ and radius of the circular pore opening r (25, 26):

$$2R_{ac} = \frac{1}{2\sigma r}. \qquad (5)$$

A comprehensive theoretical treatment of diffusion-limited ion transport through ionic channels giving generalization of the access resistance notion for the case of ion-selective pores was developed by Laüger (27). Later, in experiments with highly cation-selective gramicidin A channels (28), it was shown that aqueous diffusion limitations may be an important determinant of the channel permeability characteristics. Gramicidin single-channel current-voltage characteristics at low permeant ion concentrations exhibited voltage-independent limiting currents consistent with a diffusion-controlled process. In what follows, we show the possibility of direct measurement of access resistance of ohmic nonselective pores with the use of water-soluble polymers.

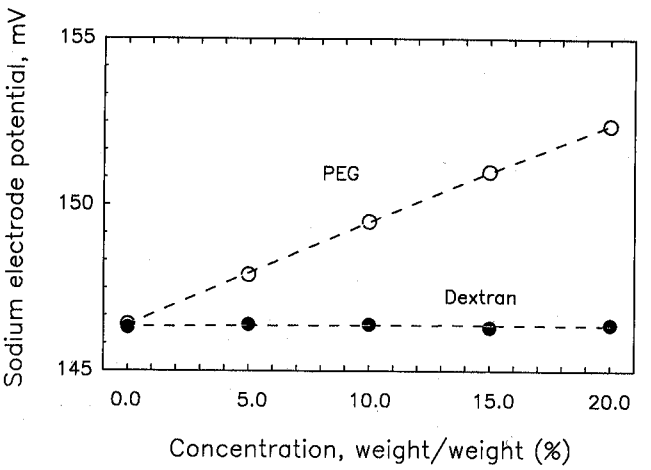

FIGURE 9 A sodium electrode potential as a function of the polymer concentration. PEG 400 increases sodium activity due to binding of water molecules. Dextran does not change sodium ion activity. Note that polymers were added to a stock solution of 1 M NaCl. In this case the number of water molecules per salt ion is the same for all points in the graph.

Suppose that a given addition of PEG to a NaCl bathing solution decreases the resistance of the channel proper to the same degree for every channel level. The measured difference then may be attributed to the access resistance "interference." Indeed, larger channels have larger contributions of the access resistance. This follows because the resistance of the channel proper is expected to decrease as the inverse radius squared, but the access resistance decreases only as the inverse radius. Thus, the hypothetical increase in conductance of the channel proper should be more damped for higher conductance levels (compare curves in Fig. 4).

What is the reason for the channel conductance rise for nonpenetrating PEGs? Polyethylene glycols bind several molecules of water per polymer chain and order several more in their vicinity (29, 30). Thus, PEG competes with ions of electrolyte for water molecules. This has the effect of increasing the activity of ions in solution. In other words, the action of PEG cannot be regarded as simply taking up space, but it also induces a local ion concentration increase.

To estimate the value of this effect, we measured the activity of sodium in polymer-containing solutions using a sodium-sensitive electrode (sodium combination electrode; Fisher Scientific, Pittsburgh, PA). Fig. 9 shows a substantial increase in salt activity in the presence of PEG. The value of the effect is close to that obtained for channel conductance. Calibration of the sodium electrode with NaCl solutions showed that 15% of PEG in 1.0 M solution gives the same electrode potential as 1.17 M polymer-free NaCl solution. A relative increase in electrolyte conductivity is 1.14. The corresponding value for 20% of PEG concentration is 1.18. It is interesting to

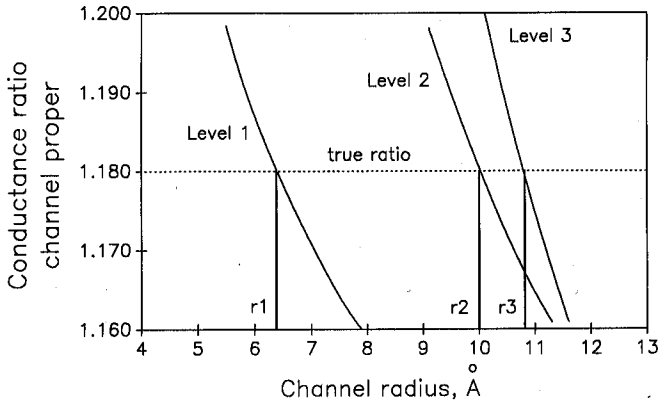

FIGURE 10 Channel proper conductance ratio, h^*_{pn}/h_{pn}, corrected on the channel access resistance as a function of the channel radius in 20% of PEG 17,000 solution. True ratio of 1.18 is expected on the basis of increase in salt activity, measured by sodium electrode (Fig. 9). Bars *r1*, *r2*, and *r3* show values of the channel radii at the corresponding conductance levels.

note that equal amounts of dextran 17,900 do not produce a measurable increase in sodium activity.

In the polymer-free solution, the measured channel conductance h_{mn} for each level n may be written to include explicitly the conductance of the channel proper and the access conductance:

$$\frac{1}{h_{mn}} = \frac{1}{h_{pn}} + \frac{1}{2\sigma r_n}, \tag{6}$$

where h_{pn} is the conductance of the channel proper (level n), and r_n is the radius of the channel in state n. The same equation should apply in the case of the polymer-containing solutions

$$\frac{1}{h^*_{mn}} = \frac{1}{h^*_{pn}} + \frac{1}{2\sigma^* r_n}, \tag{7}$$

where symbols with an asterisk stand for the same values as in Eqs. 5 and 6 but measured in or defined for experiments with polymers.

The conductance ratios for the channel proper may be expressed as functions of channel radii, using experimentally obtained conductances and solution conductivities:

$$\frac{h^*_{pn}}{h_{pn}} = \frac{2\sigma r_n - h_{mn}}{2\sigma^* r_n - h^*_{mn}} \frac{\sigma^* h^*_{mn}}{\sigma h_{mn}}. \tag{8}$$

Thus, the corrected conductance ratio for each level can be plotted as a function of the corresponding radius. The results for 20% concentration of PEG 17,000 are shown in Fig. 10. Intersections of curves with conductance ratio 1.18 corresponding to the increase of "local" electrolyte conductivity give channel radii at different conducting levels.

A similar procedure may be used for dextran data. As it follows from Fig. 9, addition of dextran does not change electrolyte activity and, therefore, its local conductivity. Then, the conductances of the channel proper in different states should not change in the presence of nonpenetrating dextran and the corrected conductance ratio equal to 1.00 should be used for radius evaluation. Fig. 11 illustrates results for 15% dextran concentration. A reasonable agreement between channel radii obtained from experiments with such different water-soluble polymers as water-binding polyethylene glycol and "inert" dextran permits us to conclude that access resistance considerations may be regarded as a useful tool for channel sizing.

Using Eqs. 5–7, we may write the value of the access resistance in polymer-free solution in the form:

$$2Rac = \frac{\sigma^*}{\sigma h^*_{mn}} \frac{h^*_{pn}/h_{pn} - h^*_{mn}/h_{mn}}{h^*_{pn}/h_{pn} - \sigma^*/\sigma}, \tag{9}$$

Thus, measuring channel conductance h_{mn} and solution specific conductivity σ in polymer-free solution and corresponding values, i.e., h^*_{mn} and σ^*, in solution with added nonpenetrating polymer, we can calculate the channel access resistance $2Rac$. The radius at a given state n is then given according to

$$r_n = \frac{h^*_{mn}}{2\sigma^*} \frac{h^*_{pn}/h_{pn} - \sigma^*/\sigma}{h^*_{pn}/h_{pn} - h^*_{mn}/h_{mn}}, \tag{10}$$

where conductances of the channel proper, i.e., h_{pn} and h^*_{pn}, enter only as a ratio. For water-binding polymers, this ratio may be obtained experimentally using salt activity measurements; for dextrans, according to Fig. 9, this ratio is always equal to unity. Table 1 summarizes averaged data for different polymers at two concentrations. Apparent channel radii at different levels and mean access resistances are presented in Table 2, together with total channel resistances to show their relative values. Access resistances were measured using Eq. 9.

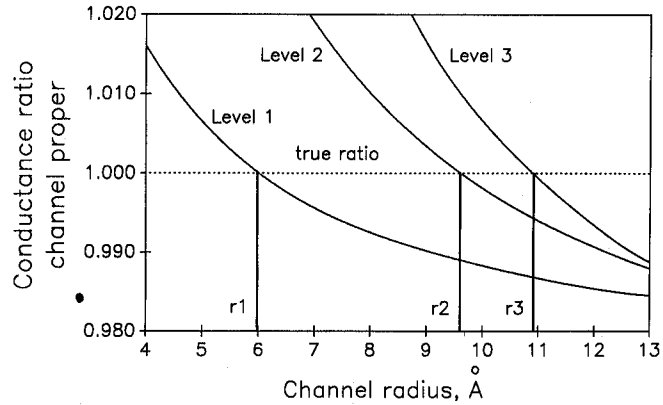

FIGURE 11 Channel proper conductance ratio, h^*_{pn}/h_{pn}, corrected on the channel access resistance as a function of the channel radius in 15% of dextran 17,900 solution. True ratio of 1.00 is used because the dextran does not change the salt activity (Fig. 9). Bars *r1*, *r2*, and *r3* show values of the channel radii at the corresponding conductance levels.

TABLE 1 **Apparent channel radii (Å) of different conducting levels derived from the channel access resistance according to Eq. 10**

	PEG 3,400		PEG 17,000		Dextran 17,900	
Concentration (%)	15	20	15	20	15	20
h^*_{pn}/h_{pn} ‡	1.14	1.18	1.14	1.18	1.00	1.00
σ^* §	4.88	3.99	4.86	3.96	5.42	4.63
Level 1 radius	6.7	7.0	6.6	6.4	6.0	5.2
Level 2 radius	11.1	10.4	11.0	10.0	9.6	9.6
Level 3 radius	12.4	10.6	12.7	10.8	10.9	11.1

‡ Ratios of conductances of the channel proper were assumed to be the same for all levels and were calculated on the basis of the salt activities measurements in the presence of polymers (Fig. 9) as described in the text. Channel conductances measured in the polymer-free solution were h_{m1} = 0.67 nS, h_{m2} = 1.62 nS, and h_{m3} = 2.63 nS.

§ Bulk conductivity of the polymer-containing solution σ^* is given in S/m units, σ = 8.1 S/m.

When deriving Eqs. 9 and 10, we assumed the alamethicin channel to be an ohmic, nonselective pore. This assumption is in good agreement with the data reported in literature. Most groups mention linear (8, 10) or even "very linear" (14) behavior of the channel current at voltages up to 125 mV. The selectivity of the channel is claimed to be very poor. Due to a high sensitivity of the alamethicin-induced conductance to voltage, direct measurements of selectivity by conventional methods is difficult if not impossible. Existing data on alamethicin channel selectivity are obtained by different extrapolation methods. In our opinion, the most reliable measurements are those of the single-channel conductance in different chloride salts with varying cation size (31, 32). It was shown that the channel conductance at a particular level is exactly proportional to bulk solution conductivities for a number of small cations, sodium cation included. It is obvious that such a proportionality may hold only for a nonselective pore. These features of alamethicin channel justify our simplified approach. A channel with a nonlinear, current-voltage relationship is considered in the Appendix.

Channel radii in different conducting states also may be estimated in a traditional way from the "total" single-channel conductance h_{mn} if the conductance of the channel proper in Eq. 6 may be written as $\pi r_n^2 \sigma / \iota$, where ι is the channel length. The main assumption of this approach is that bulk electrolyte conductivity may be used for a description of ionic transport through the channel.

TABLE 2 **Apparent channel radii (Å) and access resistances compared with total channel resistance**

	Level 1	Level 2	Level 3
Total channel resistance (R_t, MΩ)	1,490	617	380
Access resistance ($2R_{ac}$, MΩ)	98 ± 9	60 ± 3	54 ± 4
$2R_{ac}/R_t$*	0.066	0.097	0.142
Channel radius	6.3 ± 0.5	10.3 ± 0.6	11.4 ± 0.8

* Note that contribution of the channel access resistance increases with apparent channel radius.

Sources of potential errors in estimating the channel radius from channel conductance are well known (16). Most important are channel length, "bulk conductivity" of electrolyte within the channel, and deviations in the structure of the channel from assumed cylindrical geometry. Let us compare them with possible sources of errors in access resistance considerations.

Channel length is not used as a parameter in access resistance considerations, and bulk conductivity is used in the model only for the electrolyte outside the channel, so the first two error sources seem not to be significant in channel dimension evaluation. This is not true for the channel geometry; possible structure deviations from a cylinder may induce substantial corrections. For example, if the channel under study is not a single cylinder but an array of many parallel "pipes" with the same total cross-section separated from each other by several inner radius distances, the contribution of access resistance will be smaller. The access resistance will then correspond to bigger apparent channel radius, r, calculated according to Eq. 5. This is due to a different scaling of access resistance and resistance of the channel proper with radius. Although access resistance scales as inverse radius, resistance of the channel proper is expected to scale as inverse radius squared. So, access resistance measurements are sensitive to channel geometry, though for close packed pipes the overestimation of the effective channel radius should be negligible.

The most geometry-sensitive is the steric approach that allows to discriminate between cluster of pipes and single cylindrical channel of the same conductance. Let us now have a closer look at the data plotted in Fig. 5 to compare results of steric analysis with those obtained from access resistance considerations. One can see that although experimental curves for every level are distinctly different, the shift of the curves at the "half effect" conductance ratio cannot account for channel radius increase with the level number taken from Table 2. Definitely, the half effect polymer weight for level 1 is somewhere between 600 and 1,000 D, whereas for level 3 it is between 1,000 and 1,500 D (Fig. 5). Considering that the polymer hydrodynamic radius is proportional to the

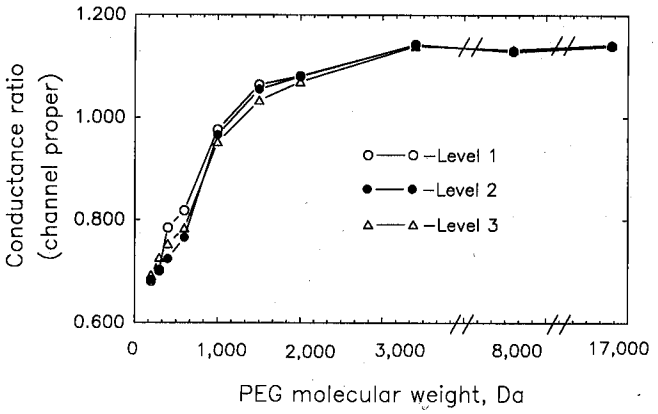

FIGURE 12 The channel proper conductance ratios for 15% of PEG of different molecular weights. This ratio is denoted as h^*_{pn}/h_{pn} in the discussion. The curves are calculated from data in Fig. 5 using the channel access resistance correction (Eq. 8).

square root of its molecular weight (15), we arrive at a conclusion that the difference between radii of the channel in levels 1 and 3 is well below of that given in Table 1.

A more rigorous consideration of steric effect should consider corrections for the channel access resistance. Fig. 12 presents the effect of polymers on conductance of the channel proper after the correction of channel access resistance was made according to Eq. 8 using average channel radii from Table 2. It can be seen that the reduction of channel conductance in all three levels follows essentially the same curve, thus suggesting that steric channel radius does not change noticeably from level 1 to level 3. These findings are in qualitative accord with the studies of alamethicin channel cation selectivity for a variety of chloride salts (14, 30) where "slit" and "sieve" models of the channel were proposed.

A comparison of data presented in Figs. 5 and 12 shows the importance of access resistance corrections for the channel radius evaluation from the "steric effect." For example, the effect of PEG 2,000 on conductance of the channel proper (Fig. 12) is the same for all three levels, suggesting a constant steric radius, whereas conductance of the system access - channel proper - access (i.e., directly measured in a reconstitution experiment) shows a significant difference.

The access resistance consideration approach, being also geometry sensitive but in a somewhat different manner, shows that the effective radius of an alamethicin channel opening grows approximately as the square root of its total conductance. This observation is in good agreement with the "barrel-stave" model (9, 33) and contradicts the case of parallel independent channels. For independent channels, the ratio of the access resistance to the total resistance (R_{ac}/R_t) is equal to that of a single channel and does not depend on the number of channels. For alamethicin channels, as one can see from Table 2, the ratio R_{ac}/R_t increases with the conductance level. We explain this by considering that pipes assembled in the channel interfere with each other via their access areas. Taken together, our findings permit us to conclude that at higher conducting levels the alamethicin channel is comprised of a closely packed "multipore" cluster.

CONCLUSIONS

The action of water-soluble polymers on amplitudes of different conducting levels of alamethicin channel may be summarized as follows.

Addition of polymers of different molecular weights in equal wt/wt concentrations decreases bulk conductivity of electrolyte solution independently on their molecular weight but influences alamethicin channel conductance in a weight-dependent way.

Measurements of the open channel noise show that the reduction of the channel conductance by small polymers is well described by the increase in microviscosity of the solution inside the channel. The characteristic times of channel "blocking" by polymer were found to be in a reasonable agreement with corresponding diffusion rates.

A novel approach incorporating the notion of access resistance was applied to data analysis. It was shown that a comparison of channel conductance in the presence of nonpenetrating polymers with that obtained in polymer-free solution may be used for the evaluation of channel dimensions independently from both steric and "total" channel conductance considerations.

From the steric considerations of the channel radii at different conductance levels and the access resistance measurements, we conclude that the alamethicin channel is a parallel array of closely packed pores of nearly uniform dimensions.

APPENDIX

In principle, the nonlinearity of the channel proper conductance may be taken easily into account. Let us consider the case where conductance of the channel proper in Eq. 6 is a function of voltage drop across the channel proper but, for simplicity, does not depend on polymer addition (as in experiments with dextran). Let us further assume that access regions are still ohmic. Then, differentiating Eq. 6 with respect to σ under the condition that the total voltage drop U in the system access - channel proper - access is held constant, we obtain relation

$$r_n = \frac{1}{2}\left(\frac{h_{mn}}{\sigma}\right)^2\left(\frac{\partial h_{mn}}{\partial \sigma}\right)^{-1}[A_n + (A_n^2 - D_n)^{1/2}]. \quad \text{(A1)}$$

Here the term in square brackets describes the relative radius correction that is due to channel nonlinearity and is defined by

$$A_n = \frac{1}{2}\left(1 + \frac{\sigma}{h_{mn}}\frac{\partial h_{mn}}{\partial \sigma} + \frac{U}{h_{mn}}\frac{\partial h_{mn}}{\partial U} - \frac{U\sigma}{h_{mn}^2}\frac{\partial h_{mn}\partial h_{mn}}{\partial \sigma \partial U}\right), \quad \text{(A2)}$$

and

$$D_n = \frac{\sigma}{h_{mn}} \frac{\partial h_{mn}}{\partial \sigma} + \frac{U\sigma}{h_{mn}^2} \frac{\partial h_{mn} \partial h_{mn}}{\partial \sigma \partial U}, \qquad \text{(A3)}$$

through the values that can be measured directly. For $\partial h_{mn}/\partial U = 0$, i.e., for linear current-voltage (I-V) channel curves, the term in square brackets equals unity, and Eq. A1 coincides with Eq. 10 for $h_{pn} = h_{pn}^*$ and $\sigma - \sigma^* \to 0$.

In the case of a superlinear I-V curve, the effect of polymer addition should be amplified by the channel nonlinearity because addition of a polymer decreases the voltage on the channel proper and, therefore, increases its resistance. This increase in the resistance of the channel proper adds to the polymer-induced increase of the access resistance. A larger apparent access resistance will result in a smaller channel radius derived from Eqs. 5 and 10, which should be corrected according to Eq. A1. For example, for $(\sigma/h_{mn})(\partial h_{mn}/\partial \sigma) = 0.1$, i.e., close to results reported in this article, and superlinearity of $(U/h_{mn})(\partial h_{mn}/\partial U) = 0.1$, the value of the correction term in Eq. A1 equals 1.089.

We are grateful to Dr. V. A. Parsegian for valuable discussions and the critical review of the manuscript and to Drs. W. W. Webb and J. Zimmerberg for useful comments.

This work was supported by grants from the Office of Naval Research.

Received for publication 19 February 1992 and in final form 14 September 1992.

REFERENCES

1. Zimmerberg, J., and V. A. Parsegian. 1986. Polymer inaccessible volume changes during opening and closing of a voltage-dependent ion channel. *Nature (Lond.)*. 323:36–39.
2. Zimmerberg, J., F. Bezanilla, and V. A. Parsegian. 1990. Solute inaccessible aqueous volume changes during opening of the potassium channel of the squid giant axon. *Biophys. J.* 57:1049–1064.
3. Sabirov, R. Z., O. V. Krasilnikov, V. I. Ternovsky, and P. G. Merzliak. 1991. Influence of non-electrolytes on ion mobility in an aqueous solution volume and in the channel cavity. Determination of pore radius from electrical measurements. *Biol. Membr.* 8:280–291. (In Russian.)
4. Bezrukov, S. M., and I. Vodyanoy. 1991. Effect of polyethylene glycols on alamethicin channel. *Biophys. J.* 59:457*a*. (Abstr.)
5. Vodyanoy, I., and S. M. Bezrukov. 1991. Sizing of ion pores in bilayer using water-soluble polymers: pore-polymer interaction problem. *Bull. Am. Phys. Soc.* 36:2015.
6. Hall, J. E., I. Vodyanoy, T. M. Balasubramanian, and G. R. Marshall. 1984. Alamethicin. A rich model for channel behavior. *Biophys. J.* 45:233–247.
7. Gordon, L. G. M., and D. A. Haydon. 1972. The unit conductance channel of alamethicin. *Biochim. Biophys. Acta.* 255:1014–1018.
8. Eisenberg, M., J. E. Hall, and C. A. Mead. 1973. The nature of the voltage-dependent conductance induced by alamethicin in black lipid membranes. *J. Membr. Biol.* 14:143–176.
9. Boheim, G. 1974. Statistical analysis of alamethicin channels in black lipid membranes. *J. Membr. Biol.* 19:277–303.
10. Latorre, R., and O. Alvarez. 1981. Voltage-dependent channels in planar lipid membranes. *Physiol. Rev.* 61:77–150.
11. Montal, M., and P. Mueller. 1972. Formation of bimolecular membranes from lipid monolayers and study of their properties. *Proc. Natl. Acad. Sci. USA.* 65:3561–3566.
12. Vodyanoy, I., J. E. Hall, and T. M. Balasubramanian. 1983. Alamethicin-induced current-voltage asymmetry in lipid bilayers. *Biophys. J.* 42:71–82.
13. Balasubramanian, T. M., N. C. E. Kendrick, M. Taylor, G. R. Marshall, J. E. Hall, I. Vodyanoy, and F. Reusser. 1981. Synthesis and characterization of the major component of alamethicin. *J. Am. Chem. Soc.* 103:6127–6132.
14. Eisenberg, M., M. E. Kleinberg, and J. H. Shaper. 1977. Channels across black lipid membranes. *Ann. N. Y. Acad. Sci.* 303:281–291.
15. Kuga, S. 1981. Pore size distribution analysis of gel substances by size exclusion chromatography. *J. Chromatogr.* 206:449–461.
16. Jap, B. K., and P. J. Walian. 1990. Biophysics of the structure and function of porins. *Q. Rev. Biophys.* 23:367–403.
17. Richmond, P., and M. Lal. 1974. A theoretical treatment of entropic repulsions by polymers. *Chem. Phys. Lett.* 24:594–596.
18. Neumcke, B. 1982. Fluctuation of Na and K currents in excitable membranes. *Int. Rev. Neurobiol.* 23:35–67.
19. Borisova, M. P., L. N. Ermishkin, and A. Ya. Silberstein. 1979. Mechanism of blockage of amphotericin B channels in a lipid bilayer. *Biochim. Biophys. Acta.* 553:450–459.
20. Van Driessche, W., and W. Zeiske. 1985. Ionic channels in epithelial cell membranes. *Physiol. Rev.* 65:833–903.
21. Bezrukov, S. M., V. G. Pokrovskii, and Yu. V. Natochin. 1986. Mechanism of stimulation of sodium channels with cobalt ions in apical membrane of frog skin cells (fluctuation analysis). *Dokl. Biophys.* 286/287/288:307–310.
22. Bezrukov, S. M., and I. Vodyanoy. 1991. Electrical noise of the open alamethicin channel. *In* Noise in Physical Systems and 1/f Fluctuations. T. Musha, S. Sato, and M. Yamamoto, editors. Ohmsha, Ltd., Tokyo. 641–644.
23. Machlup, S. 1954. Noise in semiconductors: spectrum of a two-parameter random signal. *J. Appl. Physics.* 25:341–343.
24. Verveen, A. A., and L. J. DeFelice. 1974. Membrane noise. *Prog. Biophys. Mol. Biol.* 28:189–265.
25. Hall, J. E. 1975. Access resistance of a small circular pore. *J. Gen. Physiol.* 66:531–532.
26. Hille, B. 1984. Ionic Channels of Excitable Membranes. Sinauer, Sunderland, UK. 426 pp.
27. Laüger, P. 1976. Diffusion-limited ion flow through pores. *Biochim. Biophys. Acta.* 455:493–509.
28. Andersen, O. S. 1983. Ion movement through gramicidin A channels. Studies on diffusion-controlled association step. *Biophys. J.* 41:147–165.
29. Lebovka, N. I., F. D. Ovcharenko, and V. V. Mank. 1983. Features of hydration of polyethylene oxides according to proton magnetic resonance data. *Dokl. Phys. Chem.* 268:8–11.
30. Bony, L. T., and S. W. Hui. 1987. The mechanism of polyethylene glycol-induced fusion in model membranes. *In* Cell Fusion. A. E. Sowers, editor. Plenum Press, New York. 301–330.
31. Gordon, L. G. M. 1974. Ion transport via alamethicin channels. *In* Drugs and Transport Processes. B. A. Callingham, editor. Macmillan, London. 251–264.
32. Gordon, L. G. M., and D. A. Haydon. 1975. Potential-dependent conductances in lipid membranes containing alamethicin. *Philos. Trans. R. Soc. Lond. B Biol. Sci.* 270:433–447.
33. Bauman, G., and P. Mueller. 1974. A molecular model of membrane excitability. *J. Supramol. Struct.* 2:538–557.